

## NASA's Deep Space 1 Ion Engine

John R. Brophy  
*Jet Propulsion Laboratory*  
*California Institute of Technology*  
*Pasadena, California 91109*  
[John.R.Brophy@jpl.nasa.gov](mailto:John.R.Brophy@jpl.nasa.gov)

**Ion propulsion is now a legitimate propulsion option for future deep space missions. The long journey required to get from the first laboratory test of an ion engine in 1960 to the first successful flight of an ion propulsion system on NASA's Deep Space 1 mission in 1998 is briefly summarized herein. An overview of the operation of the Deep Space 1 ion engine is provided along with a description of the complete ion propulsion system on the spacecraft. Engine performance measured in space compares well with that based on ground test data. Future deep space missions desire improved engine performance in the form of longer engine life (greater total impulse) and greater specific impulse. Derivatives of the NSTAR ion engine are being evaluated to assess their capability to meet these future needs.**

### Introduction

The first use of solar electric propulsion (SEP) on a deep-space mission began with the launch of NASA's Deep Space 1 (DS1) spacecraft on October 24, 1998 [1]. This marks a major milestone in the development of advanced propulsion for deep-space missions. The DS1 spacecraft uses a single xenon ion engine, provided by the NASA Solar electric propulsion Technology Applications Readiness (NSTAR) project, as the primary on-board propulsion system. This propulsion system can deliver a total  $\Delta V$  of 4.5 km/s to DS1 while using only 80 kg of xenon.

The NSTAR project was designed to overcome the barriers preventing the use of SEP on deep-space missions and enable ion propulsion to enter the mainstream of deep-space propulsion options. To accomplish this the project had to achieve two major objectives:

1. Demonstrate that the NASA 30-cm diameter ion engine had sufficient life and

total impulse capability to perform missions of near-term interest.

2. Demonstrate through a flight test that the ion propulsion system hardware and software could be flight qualified and successfully operated in space, and demonstrate guidance, navigation and control of an SEP spacecraft.

By all measures these objectives have been met with unqualified success. Aside from an initial hiccup [2], the operation of the NSTAR ion propulsion system on DS1 has been flawless. It successfully provided the  $\Delta V$  necessary for the July 29, 1999 flyby of the asteroid Braille, and subsequently provided the additional  $\Delta V$  required for the September 22, 2001 encounter with the comet Borrelly.

As a result of the DS1 and NSTAR projects ion propulsion is now a legitimate propulsion option for future deep-space missions [2]. The road to get to this point, however, was long and winding.

The first broad-beam, electron-bombardment ion engine was operated in the laboratory in 1960 at what is now the Glenn

Research Center [4-6]. This engine demonstrated very good performance with efficiencies as high as 70% at a specific impulse of 5500 s. The electrostatic acceleration process makes it easy to achieve attractive performance in an ion engine.

Since that time in the early 1960's the history of ion propulsion has been largely focused in three areas: achieving efficient operation at progressively lower specific impulses, scaling to other engine sizes, and achieving adequate engine life.

In the decades that followed, technologists led primarily by the Glenn Research Center were wildly successful in the first two areas. Today's ion engines are the most efficient electric propulsion devices in the specific impulse range attractive for deep space missions ( $\geq 3000$  s), and efficient ion engines have been successfully scaled an order of magnitude in diameter in both directions from Kaufman's original 10-cm diameter thruster. Electron-bombardment ion engines ranging from 1.3-cm diameter with an input power of 7 W to 150-cm diameter at 130 kW have been built and tested [7,8].

Demonstrating useful engine life with a low risk of wear-out failures, however, proved to be a much more difficult problem. The earliest references on ion thruster technology recognized the importance of lifetime [9,10] and much of the technology work since then has been focused on achieving acceptable engine service life.

In general the history of the development of long-life ion engines over the past three and a half decades is one characterized by a continual reduction in the voltages of thruster components subject to ion sputtering. The literature reveals a long history of component technology improvements that enable efficient thruster operation at ever lower (in magnitude) accelerator grid voltages and discharge voltages. The NSTAR ion engine, with its 24 V discharge and -180 V

accelerator grid voltage represents the latest point on this trend.

Such was the history for the past 35 years, the first six or seven years of ion engine technology development, however, told a different story. In this case the search for a long-lived cathode technology was the principal goal. In 1964 the best cathodes, the so-called thick-oxide-layer cathodes, had a demonstrated lifetime in an ion engine of about 600 hours [11]. The advent of the orificed hollow cathode and its application to ion engines in the middle of the 1960s almost immediately eliminated the cathode as a life-limiting component [12-14]. For example, all four hollow cathodes on the SERT II spacecraft launched in 1970 operated for more than 16,000 hours in space, and only stopped operating when the mercury propellant was exhausted [15].

### **NSTAR Ion Engine**

The NSTAR project involved a collaboration among JPL, the Glenn Research Center, Boeing Electron Dynamic Devices, Spectrum Astro, Inc., Moog Scientific Products, Inc., and Physical Science, Inc. The NSTAR engine has its roots in the 30-cm mercury ion engine development activities in the 1970s and the inert gas ring-cusp ion engine developments at GRC in the 1980s and early 1990s [16-23].

The ion engine consists of three major components; a discharge chamber in which the propellant ionization takes place, an ion accelerator system which extracts the ions from the discharge chamber and accelerates them to the exhaust velocity, and a neutralizer which injects electrons into the positive ion beam to provide space-charge and current neutralization.

The discharge chamber is formed from thin titanium sheet metal and includes a cylindrical section near the ion accelerator system and a conical section at the end

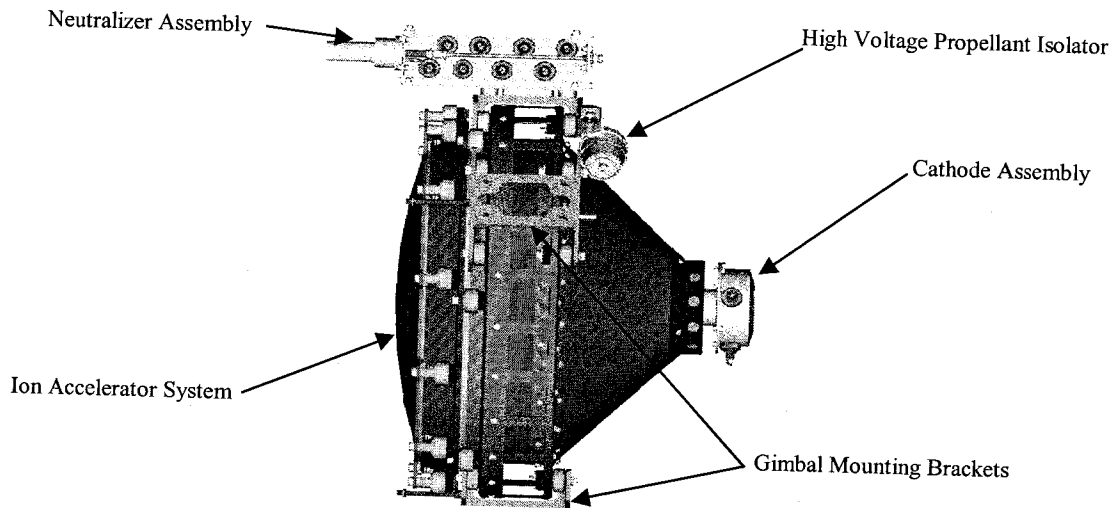


**Fig 1. Diagram of the NSTAR Ion Engine (with the plasma screen removed)**

opposite from the accelerator system as shown in Fig. 1. A DC magnetic field is superimposed on the discharge chamber to improve the ionization efficiency. Three rings of samarium-cobalt ( $\text{Sm}_2\text{Co}_{17}$ ) permanent magnets are used to form the ring-cusp magnetic field shape as suggested in Fig. 2. The cusped field configuration produces a nearly field-free region in the discharge chamber at the downstream end near the ion accelerator system. The magnetic flux density at the cusp regions adjacent to each magnet ring is of order 0.3 T, resulting in a large magnetic mirror ratio which reduces the loss of energetic electrons from the plasma. The walls of the discharge chamber serve as the anode for the DC discharge.

The NSTAR ion engine produces ions in a low-pressure DC discharge. At full power the maximum plasma density upstream of the ion accelerator system is of order  $10^{17} \text{ m}^{-3}$ . The electron temperature in the discharge chamber is of order 5 eV [24]. The density of neutral xenon atoms in the discharge chamber is of order  $10^{18} \text{ m}^{-3}$ .

A hollow cathode is used to supply electrons to the discharge. Electrons emitted by the hollow cathode are accelerated into the discharge chamber and acquire an energy that

depends on the applied voltage between the cathode and the anode. For the NSTAR thruster this voltage is typically between 24 and 26 volts. These energetic electrons both heat the electrons in the discharge chamber and ionize the propellant atoms directly. The electron energy distribution in the discharge chamber is typically non-Maxwellian. This distribution is often approximated as a Maxwellian distribution with a temperature of 5 to 6 eV plus a population of "primary" electrons with an energy close to the applied discharge voltage. Confinement of the electrons in the discharge chamber is greatly enhanced by the applied magnetic field.

The hollow cathode consists of a 6.35-mm diameter molybdenum-rhenium tube with a thoriated tungsten plate welded to the downstream end. This plate has a small orifice, of order 1 mm diameter, located on the centerline of the cathode. A porous tungsten emitter impregnated with a low-work-function barium-calcium-aluminate mixture is located inside the cathode. Electrons are emitted from this component by field-enhanced thermionic emission and travel through the orifice plate before entering the main discharge chamber.

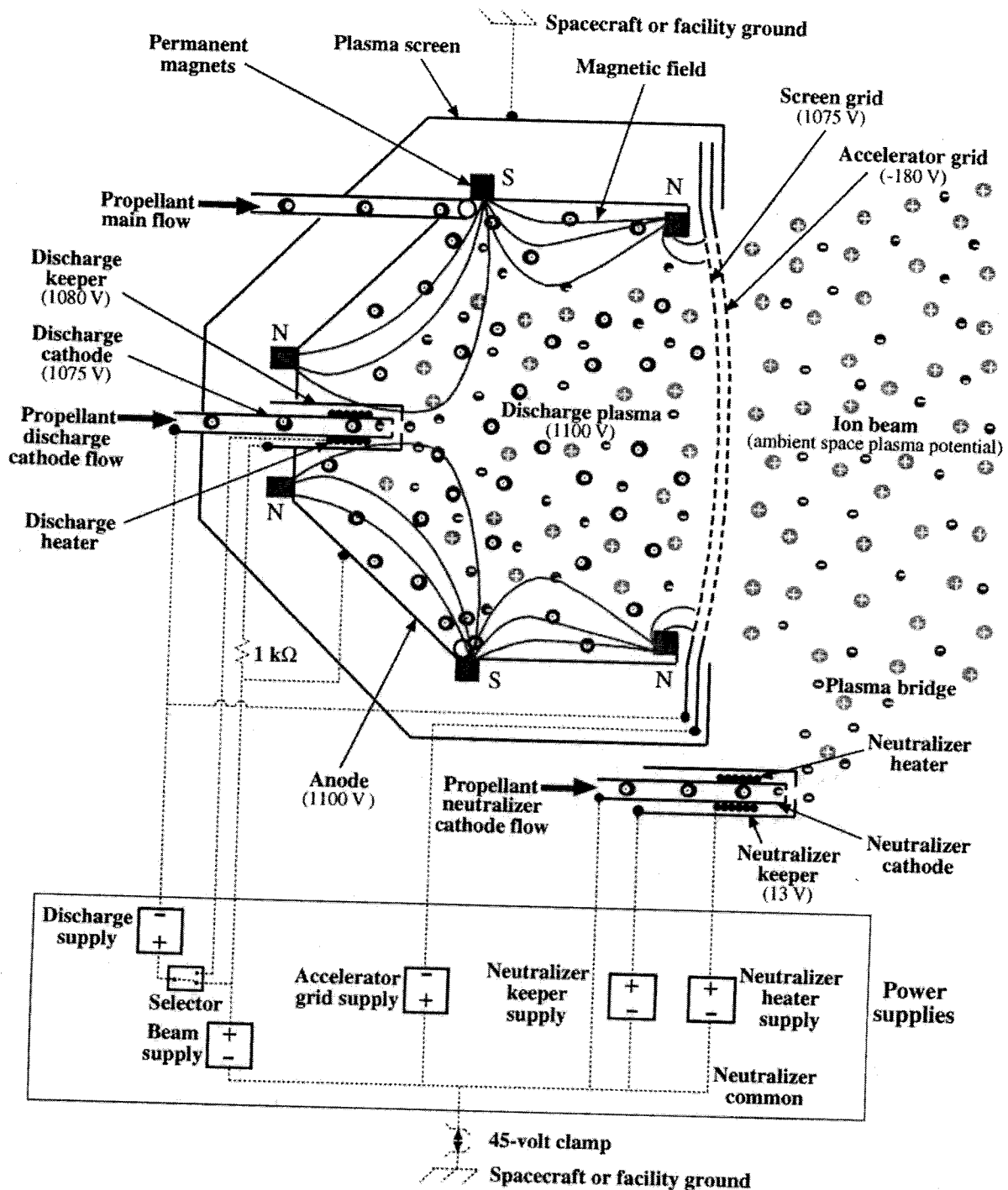


**Fig. 2 NSTAR ion engine ring-cusp magnetic field configuration.**

A small flow rate (of order 0.3 mg/s) of xenon gas is maintained through the hollow cathode resulting in the creation of a secondary plasma inside the cathode. This plasma serves to enhance the electric field at

the emitter surface and to provide a conductive path for the electrons to get from the cathode into the main discharge chamber.

Ions are created in the discharge chamber by electron bombardment. Both primary

electrons and electrons in the tail of the Maxwellian distribution contribute to the production of ions. A small fraction of multiply-charged ions is also created. The operating parameters of the NSTAR ion engine have been selected to minimize the production of doubly-charged ions since these ions are responsible for most of the erosion processes inside the discharge chamber. At full power approximately 15% of the ion beam current is in the form of doubly-charged xenon ions.

The ring-cusp magnetic field configuration produces a preferential drift of the resulting ions toward the ion accelerator system. The xenon ions are too massive to be affected directly by the applied magnetic field, but the magnetic field influences the behavior of the electrons which in turn impacts the ion behavior.

The ion accelerator system consists of two closely-spaced molybdenum electrodes with approximately 15,000 pairs of matching apertures. The apertures are formed using a chemical etching process. The inner grid is called the screen grid and is maintained at the potential of the hollow cathode, which is 1075 V positive of the neutralizer cathode at full power. The screen grid is 0.38 mm thick and the screen grid apertures are 1.91 mm diameter. The outer grid is the accelerator grid and is maintained at a voltage of 180 V negative of the neutralizer cathode. The accelerator grid is 0.51 mm thick with 1.14 mm diameter apertures. The grid separation is 0.66 mm. The negative potential on the accelerator grid is used to prevent electrons in the beam plasma from "backstreaming" into the high voltage engine. The screen grid serves to focus the ions extracted from the discharge chamber through the apertures of the accelerator grid.

Engine operation results in both radial and grid-to-grid temperature gradients. The grids of the accelerator system are spherically dished with a radius of curvature of 51 cm (20

inches) to provide the thermal-mechanical stability necessary to maintain the required grid separation with these temperature gradients. The spherical dish shape is produced using a hydroforming technique. The screen and accelerator grid blanks are hydroformed together so that imperfections in the final grid shape are reproduced in both grids resulting in a more uniform grid-to-grid separation. The grid blanks are chemically etched to form the aperture patterns after the hydroforming process. Molybdenum is used for the ion accelerator system grids because of its combination of low coefficient of thermal expansion, acceptable sputter-erosion characteristics, and the availability of chemical etching techniques.

Not all of the ions flowing toward the ion accelerator system get extracted. Some fraction of these ions strike the screen grid instead. The fraction of ions passing through the screen grid relative to the sum of these ions and those that hit the screen grid is the effective screen grid transparency to ions. For the NSTAR accelerator system, this transparency is greater than the 67% physical open area fraction of the screen grid. At full power the screen grid transparency to ions is approximately 83%.

Doubly-charged xenon ions striking the screen grid remove molybdenum atoms by sputtering. These molybdenum atoms will redeposit on other surfaces inside the discharge chamber. The walls of the discharge chamber are lined in a stainless steel wire mesh whose purpose is to contain this sputter-deposited material. The surface of the wire mesh is grit-blasted to roughen its surface and improve the adherence of the sputter-deposited films.

Since the ion accelerator system includes 15,000 apertures some of the neutral xenon gas leaks out through these apertures. The accelerator grid is designed to minimize this loss of unionized propellant and has a physical open area fraction of only 0.24. The

ratio of the mass flow rate that is exhausted in the form of ions to the total mass flow rate into the engine is called the propellant utilization efficiency.

The flux of neutral xenon atoms through the ion accelerator system results in a small production rate of charge-exchange ions in which a slow moving xenon atom exchanges an electron with an ion that was accelerated through the grids. The result is a slow moving xenon ion and a fast neutral atom. The charge-exchanged xenon ion, depending on where it is formed, may be accelerated into the negative accelerator grid. The flux of these ions to the accelerator grid results in sputter-erosion of the grid and is the major life-limiting phenomena for this electrode.

A second hollow cathode is placed outside of the main discharge chamber. This cathode, called the neutralizer, is used to inject electrons into the ion beam to provide space-charge neutralization and to prevent spacecraft charging. A flow rate of xenon gas through the neutralizer of approximately 0.3 mg/s is used to create a plasma discharge both inside the cathode and external to it. The internal plasma facilitates electron emission from the emitter surface and provides a conductive path through the cathode orifice. The external discharge forms a plasma bridge that provides a low impedance path for the electrons to get from the neutralizer to the ion beam. This plasma bridge allows the neutralizer to be physically located well outside the ion beam.

### Ion Propulsion System on DS1

The ion propulsion system provide by the NSTAR project for DS1 includes a single 30-cm diameter ion engine, a Power Processor Unit (PPU), a Xenon Feed System (XFS), and a Digital Control and Interface Unit (DCIU). A block diagram of the DS1 ion propulsion system is given in Fig. 3. Development of the

NSTAR/DS1 ion propulsion system is described in Refs. [25-28].

The PPU converts the DC solar array output power into the currents and voltages required to start and run the ion engine. It is designed operate with an input voltage in the range 80 V to 160 V in order to accommodate the variation in solar array output voltage with solar range. A block diagram of the PPU is given in Fig. 4. Details of the PPU design and development are given in [29].

The xenon feed system provides storage of the xenon propellant and controls the flow rate of xenon to the engine. Engine operation requires three separate xenon flows: the flow to the main discharge chamber, the flow through the hollow cathode in the main discharge chamber, and the flow through the neutralizer hollow cathode. The DS1 xenon feed system controls these three flow rates to  $\pm 3\%$  over the entire throttle range. The design and operation of the xenon feed system on DS1 are described in [30].

### Engine Performance

The thrust produced by an ion engine is calculated from,

$$T = \alpha F_t J_b (V_s - V_g)^{1/2} \sqrt{\frac{2M_i}{e}} \quad (1)$$

where  $J_b$  is the beam current,  $V_s$  is the beam power supply voltage,  $V_g$  is the coupling voltage between the neutralizer common and the ambient space plasma,  $M_i$  is the mass of a xenon ion and  $e$  is the charge of an electron. The factor  $\alpha$  corrects the thrust for the effect of the doubly-charged ion content of the beam and is given by,

$$\alpha = \frac{1 + (J^{++}/J^+)/\sqrt{2}}{1 + (J^{++}/J^+)} \quad (2)$$

where  $J^{++}/J^+$  is the mean ratio of doubly- to singly-charged ion beam current. For the NSTAR engine the value for  $\alpha$  is about 0.99 over the entire throttle range. The factor  $F_t$  is the thrust loss due to non-axial ion velocities,

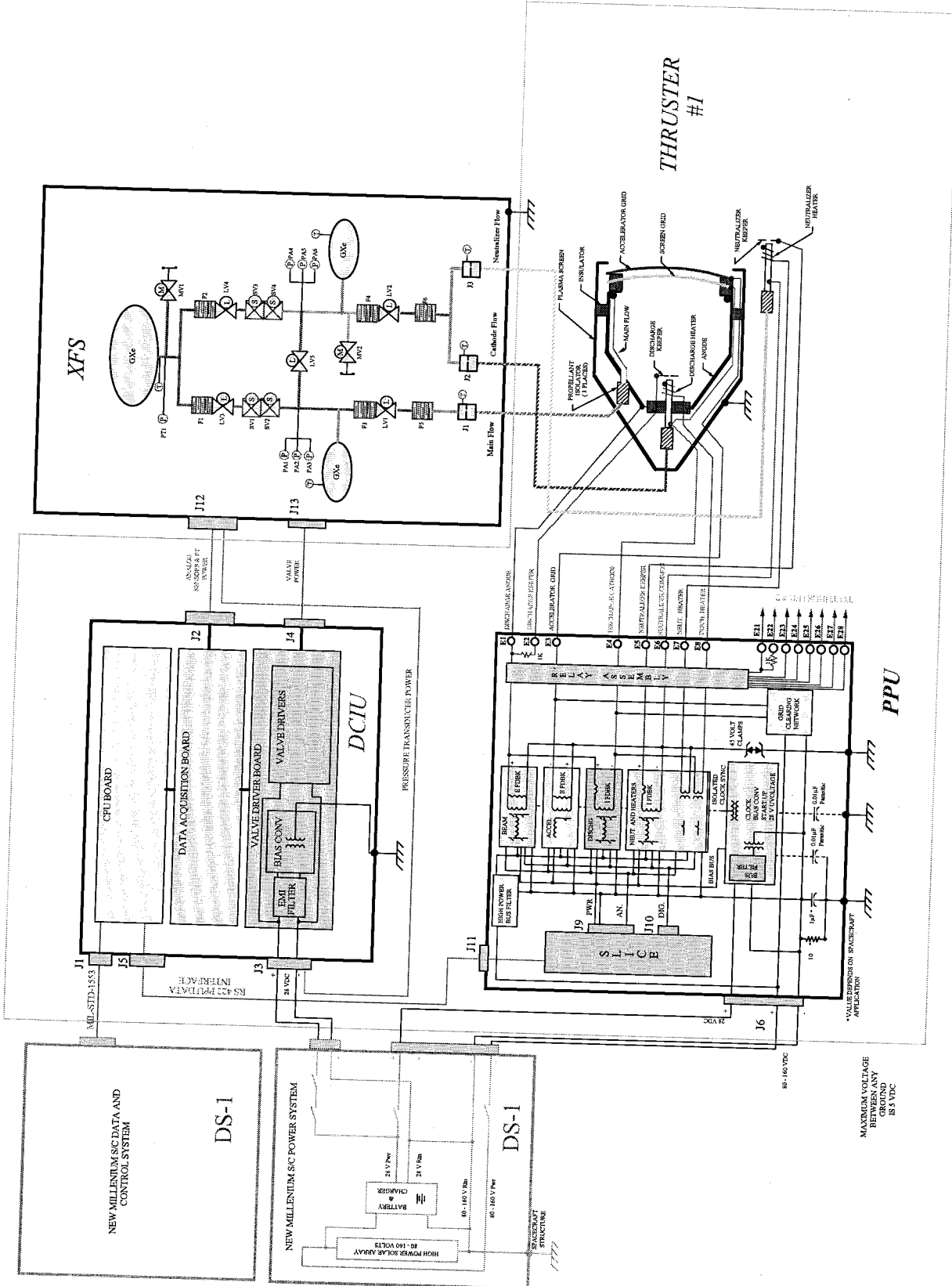


Fig. 3 NSTAR/DS1 ion propulsion system block diagram.

$$F_t = \frac{\int_{\theta_{\min}}^{\theta_{\max}} (J^+ + J^{++}) \cos \theta d\theta}{\int_{\theta_{\min}}^{\theta_{\max}} (J^+ + J^{++}) d\theta} \quad (3)$$

where  $\theta$  is the angle of the ion trajectory relative to the centerline of the thruster. For the NSTAR thruster  $F_t$  is approximated as 0.98 over the throttle range. The thrust calculated from Eq. (1) agrees with direct thrust measurements made in ground tests to within the accuracy of the thrust measurements ( $\pm 2\%$ ) [2].

During operation of the NSTAR engine on DS1 the propellant flow rates for any given throttle level are fixed by the xenon control assembly to within  $\pm 3\%$  of the nominal value. The discharge current is adjusted to maintain the desired beam current,

and the beam power supply voltage is set by the PPU. The other parameters,  $\alpha$ ,  $F_t$  and  $V_g$  in Eq. (1) do not vary significantly as the engine wears so that the thrust produced by the engine is largely unchanged over the engine's service life. However, the power required for a given thrust level increases over the engine lifetime primarily due to accelerator grid wear by charge-exchange ions [31]. This wear causes the accelerator grid apertures to get larger with time, which enables more neutral xenon gas to escape un-ionized. More discharge power is required to compensate for this reduction in neutral density in order to maintain the same beam current. To be conservative, the expected end-of-life engine performance is used in the trajectory analysis over the entire mission.

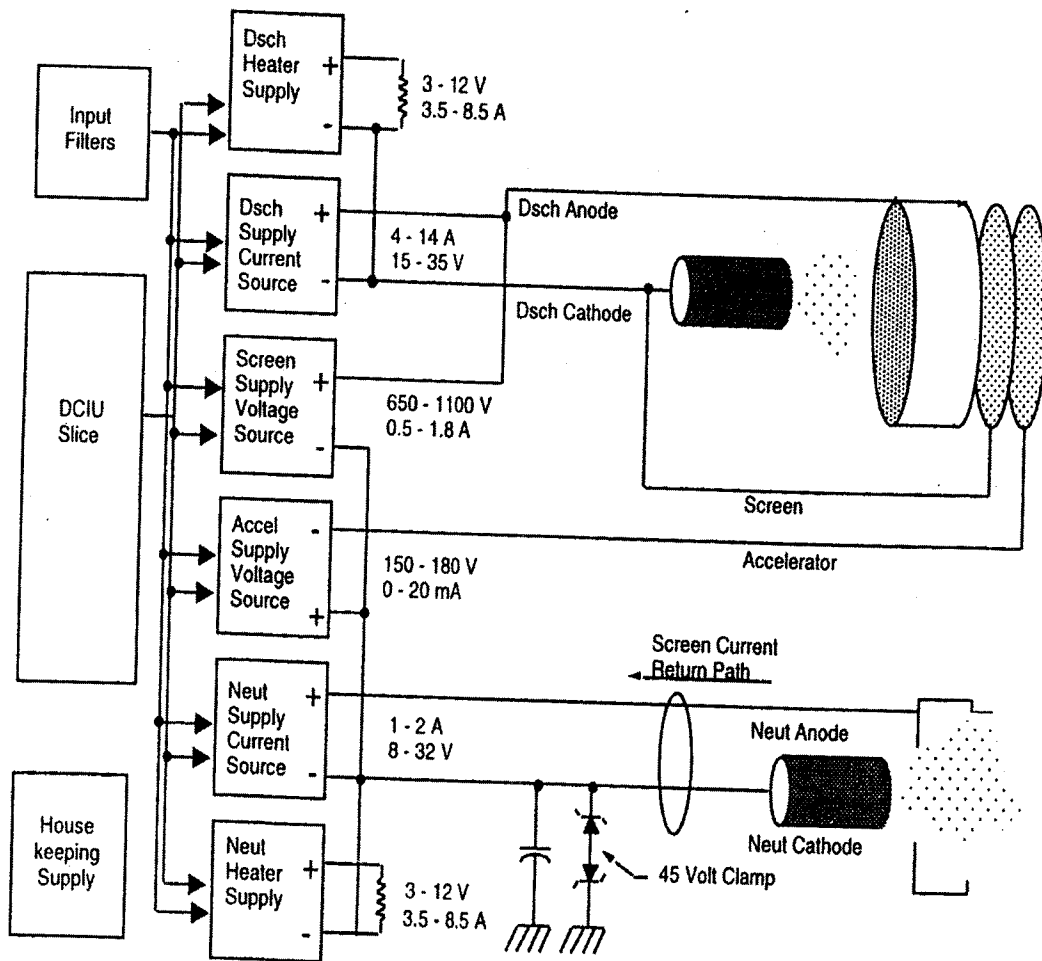


Fig. 4 PPU Block Diagram

Once the thrust is known, the specific impulse is calculated from,

$$I_{SP} = \frac{T}{\dot{m}g} \quad (4)$$

where  $\dot{m}$  is the total propellant mass flow rate and  $g$  is the gravitational constant at the Earth's surface ( $9.81 \text{ m/s}^2$ ).

The total engine efficiency,  $\eta_T$ , is defined as the ratio of the thrust power in the exhaust divided by the engine input power,  $P_E$ ,

$$\eta_T \equiv \frac{T^2}{2\dot{m}_T P_E} \quad (5)$$

### Throttling

The NSTAR ion engine is designed to be throttled over a 4.8 to 1 variation in input power with a maximum power of 2.3 kW. Power throttling is necessary in order to accommodate the variation in available solar array power with solar range for deep space missions. Throttling is accomplished by adjusting the propellant flow rate and the beam power supply voltage. At each flow rate the discharge current is adjusted to give the desired beam current for that throttle level. The NSTAR engine uses 16 discrete flow rate settings corresponding to throttle levels TH0 to TH15 shown in Table 1. This table gives the throttle levels used in the original trajectory analyses for DS1. To facilitate on-board power management DS1 subdivided the 16 throttle levels into a total of 112 "mission levels" with approximately 20 W between levels.

The 16 NSTAR throttle levels are shown graphically as the solid circles in Fig. 5 indicating the beam power supply current and voltage for each level. Fourteen of the sixteen throttle levels have the same beam supply voltage of 1100 V. For these throttle levels the power variation is accomplished by changing the beam current alone. The lowest two throttle levels (TH0 and TH1) have approximately the same beam current as TH3,

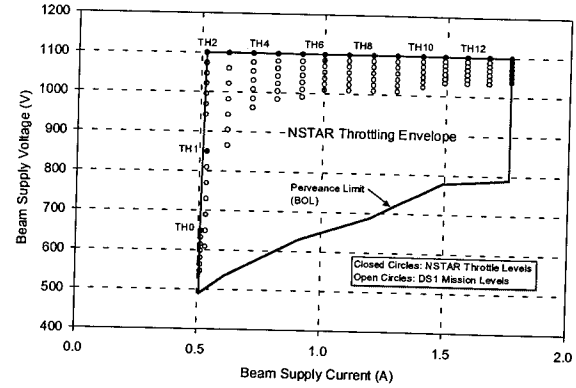


Fig. 5 NSTAR power throttling strategy.

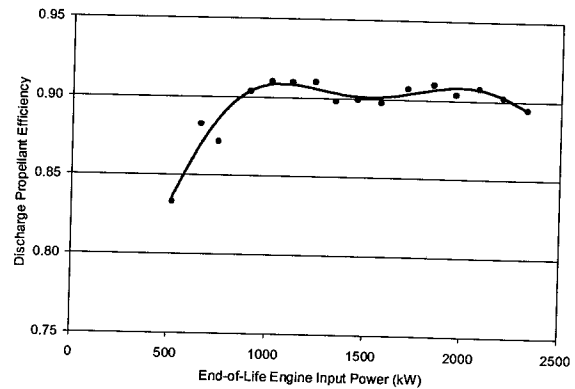
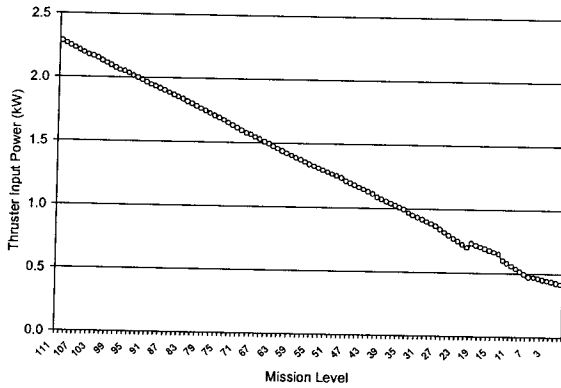


Fig. 6 NSTAR ion thruster discharge propellant efficiency is approximately constant over the throttle range except at low powers.

but reduce the beam power supply voltage to effect operation at lower powers.

At each of the 16 flow rate settings the discharge current is adjusted to produce the desired beam current. The value of the beam current for each throttle level was selected so that the discharge chamber propellant utilization efficiency is roughly constant at approximately 90% over the throttle range as shown in Fig. 6. Only at the lowest power levels is the propellant utilization efficiency allowed to decrease. This reflects the fact that the NSTAR engine's discharge chamber does not ionize the propellant as efficiently at low powers as it does at the high-power end of the throttle range.

The 112 mission levels are created by inserting six approximately 20-W throttle



**Fig. 7 NSTAR thruster input power variation over the 112 mission throttle levels used by DS1.**

steps between each of the 16 main throttle levels. The mission level throttle steps are accomplished by varying the beam power supply voltage at fixed beam current as indicated by the open circles in Fig. 6. All 112 mission levels are shown in Fig. 7.

### Operation on Deep Space 1

The ion engine on DS1 has, as of the end of August 2001, accumulated more than 13,500 hours of operation in space. This makes it by far the longest operation of any rocket engine in space. However, a good deal of this operating time has been at the low-power end of the throttling range. The thruster input power as a function of operating time during the DS1 mission is given in Fig. 8. The average thruster input power is 0.88 kW over this time.

There are two factors that have contributed to operation of the thruster at low power. First the DS1 trajectory is primarily outbound resulting, as expected, in lower power available for the propulsion system.

Second, the stellar reference unit on DS1 failed in November 1999. In the efforts to recover from this failure significantly more hydrazine attitude control propellant was used than would have been the case without the failure. Consequently, even though the DS1 operating team successfully implemented new

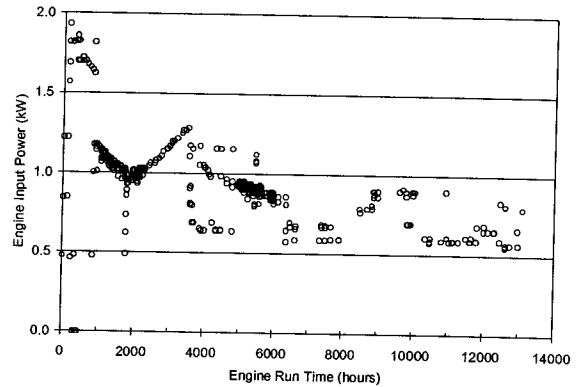
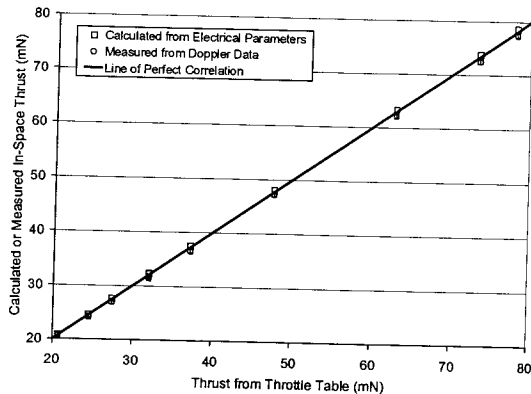


**Fig. 8 Ion engine input power history over the first 13,000 hours of operation on DS1. The average engine power is approximately 0.88 kW.**

flight control software using the MICAS camera as the stellar reference unit, there was insufficient hydrazine left on-board to maintain attitude control of the spacecraft until the September 2001 encounter with the comet Borrelly.

This problem was solved by using the ion propulsion system for attitude control. The ion engine is mounted to a two-axis mechanical gimbal that allows the ion propulsion system to perform pitch and yaw control of the spacecraft during ion engine thrusting. Roll control of the spacecraft is still performed with the hydrazine system, but the amount of propellant required for roll control is small. The use of the ion engine for attitude control saves enough hydrazine to enable the comet rendezvous. Enough control authority is obtained with the ion engine operating at the low end of the throttle range, so when the ion engine is operated solely for attitude control it is operated at low power. This maximizes the power available to the rest of the spacecraft and minimizes the use of xenon propellant.

Since the recovery from the stellar reference unit failure, which was completed in July 2000, until now (September 2001) the ion propulsion system has been operated with a duty cycle of approximately 99%. The only times the ion engine is off is when the



spacecraft is turned either to point the high gain antenna at Earth or back to its cruise attitude.

### In-Space Thrust Measurement

Direct thrust measurements were made on DS1 using radio navigation techniques [32]. In Fig. 9 the directly measured thrust is compared to that calculated using Eq. (1) with values of the beam current and voltage measured on DS1 and to the thrust values from the throttle table. It is clear that the in-space performance agrees well with both the calculated values and the expected performance. Closer inspection, however, indicates that the in-space thrust measurements may be 1 % to 2 % lower than the calculated values. The explanation for this slight difference is still being evaluated.

### Service Life Validation

Validation of the service life and failure risk for the NSTAR ion engine is established through a combination of long-duration tests and probabilistic analyses of the principal engine wear-out failure modes. This approach is essential since it is not practical to establish a low engine failure risk by testing alone. Understanding and modeling the physics of the principal failure modes provides the foundation from which the service life is established. In this approach the purposes of long duration testing are to:

1. Identify previously unknown failure modes, and to provide information to eliminate analysis oversights or errors.
2. Characterize the parameters that drive the results of the analyses.
3. Characterize the engine performance as a function of time.

The key to success in establishing the engine service life is to capture all of the key failure modes. Over the course of the NSTAR project (including the operation on DS1) more than 44,000 hours of NSTAR ion engine operation have been accumulated [33-41]. This extensive operating experience gives high confidence that all of the principal failure modes are known.

On the basis of several long-duration ground tests performed during the NSTAR project together with the body of knowledge on ion engine wear-out phenomena accumulated prior to the NSTAR project, the following list is believed to represent the top six wear-out failure modes for the NSTAR engine [41]:

1. Electron-backstreaming due to enlargement of the accelerator grid apertures.
2. Grid shorting by flakes too big to be cleared by the NSTAR grid clearing circuit.
3. Neutralizer orifice plate erosion.
4. Main cathode/keeper erosion.
5. Accelerator grid failure due to direct ion impingement from defocused beamlets caused by flakes of material on the screen grid.
6. Depletion of the cathode low work function material.

The original engine design life corresponded to a propellant throughput capability of 87 kg. The present service life guideline for the use of the NSTAR ion engine on Discovery missions which corresponds to a low probability of failure is a xenon propellant throughput of 130 kg [42]. The ion engine on DS1 has, as of the

beginning of September 2001, processed approximately 62 kg of xenon. The flight spare ion engine from DS1 is being used in an on-going life test that began in October 1998 [36]. This engine has been accumulated (at the beginning of Sept. 2001) more than 18,600 hours of operation and has processed more than 152 kg of xenon. This corresponds to 175 % of the original engine design life. Significantly, the engine continues to run well, with all of the known failure modes still apparently far from causing engine failure. The engine efficiency as a function of engine power and run time is given in Fig. 10 over the first 17,000 hours of this test. It is both clear and remarkable that there has been little change in engine performance over this time.

### Future Developments

It was anticipated early in the NSTAR project that if it were successful there would be an immediate demand for improved performance. The NSTAR project and the flight test on DS1 were highly successful and there is now a strong desire for improved engine performance. The performance parameter that most potential users would like to have improved is the engine service life [43,44]. As discussed above, the NSTAR

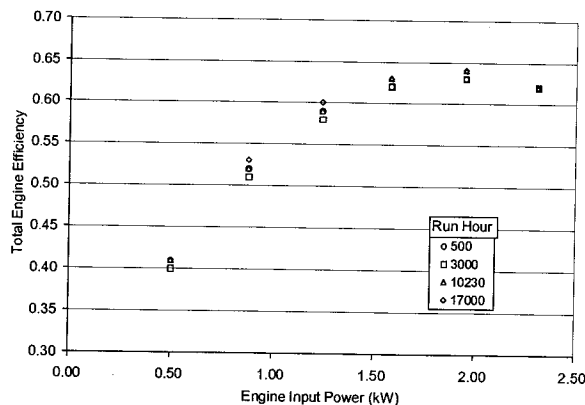


**Fig. 10** There has been little change in the DS1 flight spare ion engine over 17,000 hours of operation (corresponding to a throughput of 151 kg of xenon).

project goal for the engine service life was a propellant throughput capability of 87 kg of xenon. The throughput guideline was subsequently increased to 130 kg on the basis of successful long-duration testing and probabilistic analyses of the main failure modes. Now future users would like to have a throughput capability approaching 200 kg.

The success of DS1 has also stimulated interest in using solar electric propulsion for increasingly more difficult deep space missions, ones with characteristic velocities between 15 km/s and 20 km/s. This will require specific impulses greater than the 3100-s maximum specific impulse for the NSTAR engine.

Derivatives to the NSTAR technology are being studied to meet these needs. One is a near-term derivative, called NSTAR-2, that increases the specific impulse from 3100 s to 3700 s and increases the propellant throughput capability to 200 kg. The second derivative, called NSTAR-3 increases the specific impulse further to 5,000 s with a throughput capability of 250 kg. Larger diameter ion engines are also being developed [45].

### Conclusions

The NSTAR ion engine is the first ion engine ever used on a deep space mission. Two major achievements of the NSTAR project have made ion propulsion a legitimate option for future deep space missions. The first, and most visible, is the highly successful flight test of this ion engine on NASA's Deep Space 1 mission. This flight test has convinced mission planners that solar electric propulsion based on the NSTAR ion engine can be applied to future deep space missions with acceptable risk and cost. As a result the enormous propulsion capability of ion propulsion is now available to benefit these future missions.

The second achievement of the NSTAR project is the equally successful service life validation activity. Prior to the NSTAR project, no ion engine intended for primary propulsion had ever been operated for its full design life. The NSTAR service life validation activity successfully demonstrated 100 % of the engine design life, and more importantly developed probabilistic models of the principal engine wear-out failure modes which were used to establish an engine service life guideline of 150 % of the design life for use in NASA's Discovery class missions. On-going life testing of the Deep Space 1 flight spare ion engine has subsequently demonstrated 175 % of the original engine design life and is still running well as of this writing (Sept. 2001).

### Acknowledgement

The author sincerely thanks all of the people whose expertise and dedication made the flight demonstration of the ion propulsion system on DS1 such a fantastic success.

The work described in this paper was conducted, in part, at the Jet Propulsion Laboratory, under a contract with the National Aeronautics and Space Administration.

### References

1. Rayman, M. D., Varghese, P., Lehman, D. H., and Livesay, L. L., "Results From the Deep Space 1 Technology Validation Mission," IAA-99-IAA.11.2.01, presented at the 50<sup>th</sup> International Astronautical Congress, Amsterdam, The Netherlands, October 1999.
2. Polk, J. E., et al., "Validation of the NSTAR Ion Propulsion System on the Deep Space One Mission: Overview and Initial Results," AIAA 99-2274, presented at the 35<sup>th</sup> AIAA/ASME/SAE/ASEE Joint Propulsion Conference, Los Angeles, CA, June 1999.
3. Brophy, J. R., et al., "Ion Propulsion System (NSTAR) DS1 Technology Validation Report," JPL Publication 00-10, October 2000.
4. Kaufman, H. R., "An Ion Rocket with an Electron-Bombardment Ion Source," NASA TN D-585, 1961.
5. Kaufman, H. R. and Reader, P. D., "Experimental Performance of an Ion Rocket Employing an Electron-Bombardment Ion Source," Paper # 1374, American Rocket Society, Inc., 1960.
6. Reader, P. D., "Experimental Effects of Scaling on the Performance of Ion Rockets Employing Electron-Bombardment Ion Sources," presented at the National IAS-ARS Joint meeting, Los Angeles, CA, 1961.
7. Micronewton thruster reference AIAA-67-081, 1967
8. Nakanishi, S. and Pawlik, E. V., "Experimental Investigation of a 1.5-m-diam. Kaufman Thruster," *J. Spacecraft*, Vol. 5, No. 7, July 1968.
9. Reader, P. D., "Investigation of a 10-Centimeter-Diameter Electron-Bombardment Ion Rocket," NASA TN D-1163, January 1962.
10. Kerslake, W. R., "Accelerator Grid Tests of an Electron-Bombardment Ion Rocket, NASA TN D-1168, February 1962.
11. Kerslake, W. R., "Cathode Durability in the Mercury Electron-Bombardment Ion Thruster," AIAA-64-683, presented at the 4<sup>th</sup> Electric Propulsion Conference, Philadelphia, PA, August 1964.
12. Rawlin, V. K. and Kerslake, W. R., "SERT II: Durability of the Hollow Cathode and Future Applications of Hollow Cathodes," *J. Spacecraft*, Vol. 7, No. 1, Jan. 1970.
13. Mantieniaks, M. A., "Mercury Ion Thruster Component Testing," AIAA 79-2116, 1979.
14. Sarver-Verhey, T. R., "28,000 Hour Xenon Hollow Cathode Life Test

- Results," NASA CR-97-206231, Nov. 1997.
15. Kerslake, W. R. and Ignaczak, L. R., "Development and Flight History of SERT II Spacecraft," NASA TM 105636 (also AIAA 92-3516), July 1992.
  16. King, H. J., Poeschel, R. L., and Ward, J. W., "A 30-cm, Low-Specific-Impulse, Hollow-Cathode Mercury Thruster," *J. Spacecraft*, Vol. 7, No. 4, April 1970, pp 416-421.
  17. Bechtel, R. T., "Performance and Control of a 30-cm-diam, Low-Impulse Kaufman Thruster," *J. Spacecraft*, Vol. 7, No. 1, January 1970, pp 21-25.
  18. Bechtel, R. T. and Rawlin, V. K., "Performance Documentation of the Engineering Model 30 cm Diameter Thruster," NASA TM X-73530, November 1976.
  19. Bechtel, R. T., "The 30cm J Series Mercury Bombardment Thruster," AIAA 81-0714, presented at the 15<sup>th</sup> International Electric Propulsion Conference, Las Vegas, NV, April 1981.
  20. Rawlin, V. K., "Operation of the J-Series Thruster Using Inert Gas," NASA TM 82977 (also AIAA 82-1929), November 1982.
  21. Sovey, J. S., "Improved Ion Containment Using a Ring-Cusp Ion Thruster," NASA TM 82990, November 1982.
  22. Patterson, M. J. and Rawlin, V. K., "Derated Ion Thrusters Design Issues," NASA TM 105576, October 1991.
  23. Patterson, M. J., Haag, T. W., and Hovan, S. A., "Performance of the NASA 30 cm Ion Thruster," IEPC 93-108, presented at the 23<sup>rd</sup> International Electric Propulsion Conference, Seattle, WA, Sept. 1993.
  24. Foster, J. E., Soulas, G. C., and Patterson, M. J., "Plume and Discharge Plasma Measurements of an NSTAR-type Ion Thruster," AIAA 2000-3812, presented at the 36<sup>th</sup> Joint Propulsion Conference, Huntsville, AL, July 2000.
  25. Rawlin, V. K., et al., "NSTAR Flight Thruster Qualification Testing," AIAA 98-3936, presented at the 34<sup>th</sup> AIAA/ASME/SAE/ASEE Joint Propulsion Conference, Cleveland, OH, July 1998.
  26. Polk, J. E., et al., "In-Flight Performance of the NSTAR Ion Propulsion System on the Deep Space One Mission," ....
  27. Christensen, J. A., "The NSTAR Ion Propulsion Subsystem for DS1," AIAA 99-2972, presented at the 35<sup>th</sup> AIAA/ASME/SAE/ASEE Joint Propulsion Conference, Los Angeles, CA, June 1999.
  28. Christensen, J. A., "Design and Fabrication of a Flight Model 2.3 kW Ion Thruster for the Deep Space 1 Mission," AIAA 98-3327, presented at the 34<sup>th</sup> AIAA/ASME/SAE/ASEE Joint Propulsion Conference, Cleveland, OH, July 1998.
  29. Hamley, J. A., et al., "The Design and Performance Characteristics of the NSTAR PPU and DCIU," AIAA 98-3928, presented at the 34<sup>th</sup> AIAA/ASME/SAE/ASEE Joint Propulsion Conference, Cleveland, OH, July 1998.
  30. Ganapathi, G. B. and Engelbrecht, C. S., "Performance of the Xenon Feed System on Deep Space One," *J. Spacecraft and Rockets*, vol. 37, No. 3, pp 392-398, May-June 2000.
  31. Polk, J. E., et al., "The Effect of Engine Wear on Performance in the NSTAR 8000 Hour Ion Engine Endurance Test," AIAA 97-3387, presented at the 33<sup>rd</sup> AIAA/ASME/SAE/ASEE Joint Propulsion Conference, Seattle, WA, July 1997.
  32. McElrath, T. P., Han, D., and Ryne, M. S., "Radio Navigation of Deep Space 1 During Ion Propulsion Usage," Paper MS00/57 presented at the 15<sup>th</sup>

- International Symposium of Spaceflight Dynamics, Biarritz, France, June 2000.
33. Patterson, M. J., et al., "2.3 kW Ion Thruster Wear Test, AIAA 95-2516, presented at the 31<sup>st</sup> AIAA/ASME/SAE/ASEE Joint Propulsion Conference, San Diego, CA, July 1995.
  34. Polk, J. E., et al., "A 1000-Hour Wear Test of the NASA NSTAR Ion Thruster," AIAA 96-2717, presented at the 32<sup>nd</sup> AIAA/ASME/ASEE Joint Propulsion Conference, Lake Buena Vista, FL, July 1996.
  35. Polk, J. E., et al., "An Overview of the Results from an 8200 Hour Wear Test of the NSTAR Ion Thruster," AIAA 99-2446, presented at the 35<sup>th</sup> AIAA/ASME/SAE/ASEE Joint Propulsion Conference, Los Angeles, CA, June 1999.
  36. Anderson, J. R., et al., "Results of an Ongoing Long Duration Ground Test of the DS1 Flight Spare Ion Engine," AIAA 99-2857, presented at the 35<sup>th</sup> AIAA/ASME/SAE/ASEE Joint Propulsion Conference, Los Angeles, CA, June 1999.
  37. Polk, J. E., Anderson, J. R., and Brophy, J. R., "Behavior of the Thrust Vector in the NSTAR Ion Thruster," AIAA 98-3940, presented at the 34<sup>th</sup> AIAA/ASME/SAE/ASEE Joint Propulsion Conference, Cleveland, OH, July 1998.
  38. Polk, J. E., Brophy, J. R., and Wang, J., "Spatial and Temporal Distribution of Ion Engine Accelerator Grid Erosion," AIAA 95-2924, presented at the 31<sup>st</sup> AIAA/ASME/SAE/ASEE Joint Propulsion Conference, San Diego, CA, July 1995.
  39. Polk, J. E., et al., "In Situ, Time-Resolved Accelerator Grid Erosion Measurements in the NSTAR 8000 Hour Ion Engine Wear Test," IEPC-97-047, presented at the 25<sup>th</sup> International Electric Propulsion Conference, Cleveland, OH, August 1997.
  40. Anderson, J. R., Polk, J. E., and Brophy, J. R., "Service Life Assessment for Ion Engines," IEPC-97-049, presented at the 25<sup>th</sup> International Electric Propulsion Conference, Cleveland, OH, August 1997.
  41. Brophy, J. R., Polk, J. E., and Rawlin, V. K., "Ion Engine Service Life Validation by Analysis and Testing, AIAA 96-2715, presented at the 32<sup>nd</sup> AIAA/ASME/ASEE Joint Propulsion Conference, Lake Buena Vista, FL, July 1996.
  42. Parker, G., "NSTAR Risk Assessment for Discovery Proposals," Interoffice Memorandum PFPO-GLP-2000-002, April 5, 2000, internal JPL document.
  43. Brophy, J. R., Garner, C. E., Polk, J. E., and Weiss, J. M., "The Ion Propulsion System on NASA's Space Technology 4/Champollion Comet Rendezvous Mission, AIAA 99-2856, presented at the 35<sup>th</sup> AIAA/ASME/SAE/ASEE Joint Propulsion Conference, Los Angeles, CA, June 1999.
  44. Brophy, J. R., "Ion Propulsion System Design for the Comet Nucleus Sample Return Mission," AIAA 2000-3414, presented at the 36<sup>th</sup> Joint Propulsion Conference, Huntsville, AL, July 2000.
  45. Patterson, M. J., "Development Status of a 5/10-kW Class Ion Engine, AIAA 2001-3489, presented at the 37<sup>th</sup> AIAA/ASME/SAE/ASEE Joint Propulsion Conference, Salt Lake City, UT, July 2001.

**Table 1** Flight throttle table of parameters used in mission analysis.

<b>NSTAR Throttle Level</b>	<b>Mission Throttle Level</b>	<b>PPU Input Power (kW)</b>	<b>Engine Input Power (kW)</b>	<b>Calculated Thrust (mN)</b>	<b>Main Flow Rate (sccm)</b>	<b>Cathode Flow Rate (sccm)</b>	<b>Neutralizer Flow Rate (sccm)</b>	<b>Specific Impulse (s)</b>	<b>Total Thruster Efficiency</b>
15	111	2.567	2.325	92.67	23.43	3.70	3.59	3127	0.618
14	104	2.416	2.200	87.87	22.19	3.35	3.25	3164	0.624
13	97	2.272	2.077	83.08	20.95	3.06	2.97	3192	0.630
12	90	2.137	1.960	78.39	19.86	2.89	2.80	3181	0.628
11	83	2.006	1.845	73.60	18.51	2.72	2.64	3196	0.631
10	76	1.842	1.717	68.37	17.22	2.56	2.48	3184	0.626
9	69	1.712	1.579	63.17	15.98	2.47	2.39	3142	0.618
8	62	1.579	1.456	57.90	14.41	2.47	2.39	3115	0.611
7	55	1.458	1.344	52.67	12.90	2.47	2.39	3074	0.596
6	48	1.345	1.238	47.87	11.33	2.47	2.39	3065	0.590
5	41	1.222	1.123	42.61	9.82	2.47	2.39	3009	0.574
4	34	1.111	1.018	37.35	8.30	2.47	2.39	2942	0.554
3	27	0.994	0.908	32.12	6.85	2.47	2.39	2843	0.527
2	20	0.825	0.749	27.47	5.77	2.47	2.39	2678	0.487
1	13	0.729	0.659	24.55	5.82	2.47	2.39	2382	0.472
0	6	0.577	0.518	20.69	5.98	2.47	2.39	1979	0.420